American Journal of Sciences and Engineering Research

E-ISSN– 2348–703X, Volume 9, Issue 3, 2026

Effects of Plantain Stem Fibres on Cassava Peels Starch-Modified Low Density Polyethylene (LDPE) Composite for use as Secondary Packaging Materials

Anene U.K[1], Anyanwu P.I[2], Chike K.O[3], Arukalam I.O[4]

Department of Polymer Engineering, Federal University of Technology, P.M.B. 1526, Owerri, Imo State, Nigeria.

Abstract: *The effects of plantain stem fibres on cassava peels starch-modified LDPE composite for use as secondary packaging materials were investigated. The plantain stem fibres (PSF) and cassava peels starch (CPS) were processed to powdered form, and were characterized using Fourier transform infrared (FTIR) spectroscopy, differential scanning calorimetry (DSC) and thermo gravimetric analysis (TGA). FTIR analysis of the PSF and CPS revealed presence of cellulose, hemicellulose, and lignin. The DSC and TGA thermal analyses results showed that the PSF exhibited good thermal properties. It was further observed that the lignin component of PSF did not decompose, but the hemicellulose and cellulose content decomposed at 185.27 ^{o}C. The TGA results indicated that the pulverized CPS remained thermally stable up to 492.78 °C. The mechanical properties – tensile, compressive and flexural properties of the composite samples were conducted using a universal testing machine. Shore D hardness was conducted using a Durometer. Consequently, the tensile, flexural, and compressive strengths of the composites were observed to increase with PSF. The hardness values of the composites fall within the range of 42 and 49, which is relatively good. The linear coefficient of thermal expansion values of the composite samples were found to be low, ranging from 12.658 x 10^{-06} to 46.774 x 10^{-06} /^{o}C, making them less prone to thermal expansion and contraction. Gravimetric determination of water and oil absorptions displayed low percent water and oil absorptions. Considering the obtained results, the composite samples could serve satisfactorily as secondary food packaging materials.*

Keywords*: Cassava peels starch; Composites; Low Density Polyethylene; Plantain stem fibres; Secondary packaging materials.*

I. Introduction

Growing consumer expectations, regulatory requirements, and industrial demands have intensified the need for packaging materials capable of maintaining product quality while reducing environmental and health impacts. As these demands evolve, there is increasing pressure for packaging options that are not only reliable and safe, but also sustainable and resource efficient. In this wise, secondary food packaging which refers to the outer packaging that contains primary packaged food products provides additional protection, convenience, and marketing appeal. It protects primary packages from damage, contamination, and environmental factors (Marsh and Bugusu, 2007).

However, usage of non-biodegradable materials for the various packaging applications has raised environmental pollution concerns (Khalil et al., 2016 ; Nurul et al., 2016). Food packaging accounts for the biggest growing sector within the synthetic plastic packaging market domain (Attaran, et al., 2015; Cazón et.al., 2017; Muller et al., 2017). Large amounts of different materials, like paper, glass and plastics, are used globally

 Received-25-03-2026 Accepted- 18-06-2026

to manufacture packaging materials and more than two thirds are used in the food sector alone. This amount is growing unceasingly as a result of changes occurring in habits of food preparation and consumption, as well as the positive development of various areas and markets in the world. The packaging industry consumes the highest volumes of plastics produced globally and is the main source supplying waste plastics into the environment at an alarming rate (De Kock et al., 2020).

As demand for food rises, so does the demand for food packaging materials. Packaging materials need to be tailored to be able to maintain the quality of product as well as other rising demands from the consumers, producers, as well as legislative forces. Such demands have grown very dynamic, with calls not only for the best quality of product, but also for that product to be delivered using a sustainable packaging that imposes less impact on the health of consumers as well as the environment.

On account of this, the packaging industry is now in pursuit of biodegradable and compostable packaging that is lightweight for reducing materials use, waste, transportation costs and lower greenhouse gas emissions while supporting responsible resource utilization (Afshar et al., 2024). Plastics from biopolymers are promising to fulfil this requirement. For non-contact food packaging application, secondary packaging is used. Secondary packaging influences consumer purchasing decisions through branding, labeling, and visual appeal (Silayoi and Speece, 2007). Biodegradable packaging material is sustainaible because it is eco-friendly, recyclable, and enhances consumer convenience (Rundh, 2005).

Although significant progress has been made in the development of biopolymer-based packaging materials, challenges persist in balancing environmental sustainability, cost effectiveness, and packaging performance (Grujić et al., 2017). Natural polymers and their blends remain promising alternative due to their abundance, biodegradability, low cost, and flexible processing characteristics, offering opportunities to tailor packaging properties to specific applications (Aliotta et al., 2019; Scarfato et al., 2015). Biodegradation driven by heat, moisture, and microbial activity enables these materials to break down into simpler compounds with minimal environmental burden (Ashok et al., 2016; Peelman et al., 2013).

In view of the above, cassava starch has been widely explored for bioplastic production, including through blending with natural or synthetic polymers to enhance mechanical and thermal performance (Abotbina et al., 2022; Gómez-Bachar et al., 2024; Matheus et al., 2023; Mueller et al., 2024). However, comparatively, few studies have focused on starch-rich cassava by-products such as cassava peels, which represent the major solid residue of cassava processing and account for more than 5% of root mass (Matheus et al., 2023; Zhang et al., 2024). Research by Dasumiati et al. (2019) demonstrated that cassava peel-based bioplastics reinforced with chitosan can achieve improved tensile and thermal properties, further supporting their potential for food packaging applications. On the other hand, potato peels represent another under-utilized agro-industrial by-product rich in bioactive compounds, including phenolics and glycoalkaloids with notable antioxidant and antimicrobial activities. Their valorization has been explored in various sectors, including bioethanol and biobutanol production, underscoring their potential as a lignocellulosic resource (Hijosa-Valsero et al., 2018). Likewise, plantain stem fibres and eggshell powder present abundant, low-cost waste materials with high cellulose and calcium carbonate content, making them promising alternative for use as reinforcement biofillers in biodegradable polymer matrices.

Given the urgent need for environmentally sustainable packaging solutions and the abundance of these agricultural residues, further exploration of non-edible cassava and potato peels, plantain stem fibres, and eggshell powder as biofillers is needed. Understanding their chemical structure and thermal behaviour is essential for evaluating their compatibility with bio-based composite systems.

Therefore, this study seeks to investigate the effect of plantain fibre on cassava starch-low density polyethylene composite for us as sustainable secondary packaging materials.

II. Experimental section

2.1 Materials

The low density polyethylene (LDPE) used as a base material was obtained from the Polymer Engineering Laboratory, Federal University of Technology Owerri, Imo State. Cassava peels were procured locally from cassava processing sites in Owerri, Imo State. Then, they were washed thoroughly with clean water before shredding to small pieces. The shredded cassava peels were soaked in water for about 15 minutes and later placed in a mixing blender for grinding. This was followed by filtration, decantation and drying at 60 ^{o}C for one hour to have it in powdered form using a 75 µm mesh sieve. It was then stored in a dessicator prior to use. On the other hand, the waste plantain pseudo-stems were harvested from plantain plantation. The pseudo-stems were initially cut into pieces of about 60 cm length and then scraped with a knife to separate the fibres. The extracted fibres were subsequently washed with clean water, and sun-dried for one week. Thereafter, they were mixed with 2 g glycerol and oven-dried at 60 ^{o}C for one hour. Then, the dried plantain stem fibres were pulverized, sieved with 75 µm mesh and stored prior to use. Gum Arabic was used as a compatibilizer or bonding agent to improve the mechanical properties of the bioplastic composites.

2.2 Sample preparation

The composite samples were fabricated following the formulations given in Table 1. Firstly, each of the formulation was thoroughly mixed and homogenized using a blender. Thereafter, the different homogenized mixtures were each processed using an injection moulding machine. The temperature at the feed zone (hopper) was set 110 ^{o}C, while the temperature at the pumping zone (nozzle end) was 150 °C. The pressure was maintained at 100 psi. Consequently, flat circular samples of composite materials were produced, and kept in a cool dry place prior to characterization.

Table 1: Samples formulation involving LDPE, Cassava peel starch (CS), Plantain stem fibre and gum Arabic.

S/N	Sample Composition	Sample ID
1	100 LDPE (Virgin Sample)	VS
2	100 LDPE + 100 CS + 2 GA	BS1
3	100 LDPE + 100 CS + 10 PF + 2 GA	BS2
4	80 LDPE + 100 CS + 20 PF + 2 GA	BS3
5	60 LDPE + 100 CS + 40 PF + 2 GA	BS4
6	50 LDPE + 100 CS + 50 PF + 2 GA	BS5

2.3 Characterizations

(a) Characterization of Cassava peel starch and plantain stem fibre

(i) Fourier transform infrared (FTIR) analysis

The FTIR spectra of cassava peel and plantain stem fibre were acquired in the range of 450–4000 cm^{-1} wavenumber by use of PerkinElmer Spectrum IR spectrophotometer, version 10.7.2. The procedure involved mixing 4 mg each of the cassava peel starch and plantain stem fibre samples with 100 mg of pure anhydrous KBr. The mixture was ground to fine powdered form using a mortar and a pestle. The ground mixture was then placed onto a circular disk and pressed into a transparent flake. Subsequently, it was placed into the detection chamber of IR spectrophotometer with a sample holder, and the IR spectra were recorded with the Omnic software at a resolution of 4 cm^{-1}, with 64 scans and a gain of 1.

(ii) Gas chromatograph mass spectroscope (GC-MS)

The GC–MS chemical composition analysis of cassava peel starch and plantain stem fibre was performed using a gas chromatograph equipped with a autosampler and a mass-selective detector (Agilent, Santa Clara, CA, USA), according to the already established protocol (Becerra and Odermatt, 2013). The capillary column used was HP-5MS, 30 m × 0.25 mm × 0.25 mm, from Agilent (Santa Clara, CA, USA). Helium was used as carrier gas at 1.5 mL/min. The split–splitless injector was operated in pulsed pressure splitless mode as follows: initial

pressure 0.2 MPa (30 p.s.i.) for 1.3 min, decreased to constant flow. The purge valve was opened after 1.5 min. The injection volume was 5 µL. The temperatures of the GC system were set as follows: injector temperature 290 °C; transfer line temperature 280 °C; oven temperature program: 50 °C (1.5 min)–30 °C/min–180 °C–20 °C/min–280 °C (20 min). MS detector (quadrupole) was operated in the EI mode at 70 eV with a mass scan range of 50–450 m/z and the sampling rate of 3.6 scans/s.

(iii) Differential Scanning Calorimetry (DSC)

A small quantity of cassava peel starch and plantain stem fibre powder were taken from the bulk sample. An empty reference pan was placed on the reference side of the DSC instrument, while the sample was placed in the sample pan. Thereafter, the chamber lid was closed, and the DSC control software was opened. The essential details such as the sample mass, sample name, test parameters such as start temperature, heating/cooling rates, maximum temperature and other relevant information were entered. The file name and data storage location were entered. Following the programmed inputs, the test was initiated by clicking the start button. Thus, the DSC measured the difference in heat flow required to maintain equal temperatures between the sample and reference. This data were recorded as thermograms. Hence, the melting temperature and absorbed heat energy could be determined.

(iv) Thermogravimetric Analysis (TGA)

The mass of each of cassava peel starch and plantain stem fibre powder samples was measured, and placed on sample pan of the thermogravimetric analyzer (TGA). The TGA instrument was programmed to heat the sample from the room temperature to 1000 ^{o}C. The heating rate was set at 20 °C/minute. The test was initiated by clicking the start button on the TGA instrument. The TGA generated thermogravimetric curves which plotted the percentage of weight loss against the temperature. Thus, the oxidation and degradation temperatures were obtained.

(b) Characterization of Composite samples

To gain insight into the composite samples properties and then understand their performance during service operation, they were subjected to different characterization techniques.

(i) Microstructure analysis using Advanced Optical Microscope

A small section of the composites was cut for examination under the microscope. The mounted sample was polished using a series of abrasive papers and diamond pastes, progressing from coarse to fine grit, to achieve a mirror-like surface finish. The polished sample was etched using a sodium hydroxide solution to reveal the microstructure. The advanced software in the optical microscope was used to reveal the microstructural features such as size, shape, distribution of constituent materials. and pores observed under the microscope. The presence of pores and voids within the microstructure is critical for assessing the material's performance. thus, high porosity can lead to reduced mechanical strength and increased water absorption.

(ii) Mechanical properties analysis

The tensile properties for each sample was carried out using an electronic universal testing machine (Model: INSTRON 3369). One end of the dumb bell brake pad sample was gripped by the jaws attached to the adjustable crosshead. The tensile load (force) was hydraulically applied to the sample by pressing the start button and the magnitude of the applied load would be indicated in the input and output display unit. The load would gradually be increased until the sample breaks off and the corresponding extension recorded. From this analysis, the ultimate tensile strength, yield strength, Young's modulus, and elongation at break were obtained.

The compressive strength test for the composite samples measured the maximum compressive stress that the material can withstand before failure. Each sample was placed between the plates of the local frame. Load was applied gradually and the values of compressive strength were read on a digital device. From each formulation, three samples were tested for compressive strength and the average value was determined and recorded. However, the compressive strength (σ_C) was determined using the established equation (1):

$$\sigma_c = \frac{\mathrm{F}}{\mathrm{A}_S} \qquad (1)$$

where; F = Applied force, A_s = Cross sectional area.

Flexural test on the bioplastic composite samples was conducted via a three-point bending test using a Universal Testing Machine (UTM) to determine its flexural strength. The test evaluates how the material bends under load before breaking or reaching a specified deflection. Each of the samples was placed on a support span, and a load was applied to the center of the sample at a specified rate. As the load increased, the UTM measured the deflection of the specimen and the corresponding stress. The test was stopped when the sample got broken.

The hardness test for the composite samples is an important quality control process used to evaluate the material's resistance to deformation, which is critical for ensuring the performance and longevity of the composites. A shore D durometer, a standard method that measures the resistance of the material to indentation was used following the ASTM D2240. Each of the samples was placed on a flattened surface. The indenter of the instrument was then pressed into the sample with an applied load of 50 N for 15 seconds. The Hardness value was read from the durometer, and recorded.

(iii) Thermal Property Analysis – Linear Coefficient of Thermal Expansion

The coefficient of thermal expansion (CTE) of food packaging material is measured to ensure its dimensional stability under temperature changes, which is crucial for proper sealing, fit, and overall reliability of the packaging system over its entire temperature range. This measurement helps prevent critical failures like package deformation or seal breakage that could compromise food safety and quality, ensuring the packaging performs as designed in different environments from storage to use.

Hence, the linear coefficient of thermal expansion was measured by dilatometry method. Firstly, each of the samples' room temperature was noted. Secondly, each of the composite samples was placed in a controlled furnace. The sample was heated for 2 minutes at elevated temperature of 50 ^{o}C. Thereafter, the sample was retrieved and change in length was recorded. By measuring this change in length (ΔL) over the initial length (L_o) and the corresponding change in temperature (ΔT), the CTE (α) was calculated using equation (2):

$$\alpha = \frac{\Delta L}{L_o \times \Delta T} \quad (2)$$

(iv) Water and Oil Uptake

The determination of water and oil absorption by ASTM D570 allows for the measurement of the quantity of water and oil that are taken up by sample materials, which provides insight into how the materials perform in water-based environments or in contact with oil. Each of the composite samples was cut into 2 × 4 cm dimension and oven-dried at 60 °C. The initial weight of each of the samples was noted. The samples were immersed in water (at 25 and 50 °C) and groundnut oil (at 25 and 50 °C) for 6 hs. The weights after immersion were measured. Thus, the percentages of water and oil uptake were calculated using equation (3):

$$Water\ or\ oil\ uptake\ (\%) = \left(\frac{W_w - W_d}{W_d}\right) \times 100 \quad (3)$$

where W_w represents wet weight, while W_d = dry weight of the bioplastic composite.

III. Results and discussion

3.1 Processing of Cassava Peels and Plantain Stem Fibres

The procured cassava peels and plantain stems were processed to powdered form and fibre, respectively. Consequently, the obtained results are shown in Plate 1 and Plate 2, respectively.

Plate 1: Cassava peel powder

Plate 2: Pulverized plantain stem fibres.

The pulverized cassava peels starch obtained were fine, dry and light brown in colour. The plantain stem fibres revealed a heterogeneous mix of irregular fillers which reflects the fibrous nature of plantain stem fibres.

3.2 Fourier transform infrared (FT-IR) results

The FTIR results of the pulverized cassava peels are given in Figure 1. Figure 2 shows the FTIR spectra of the plantain stem fibres.

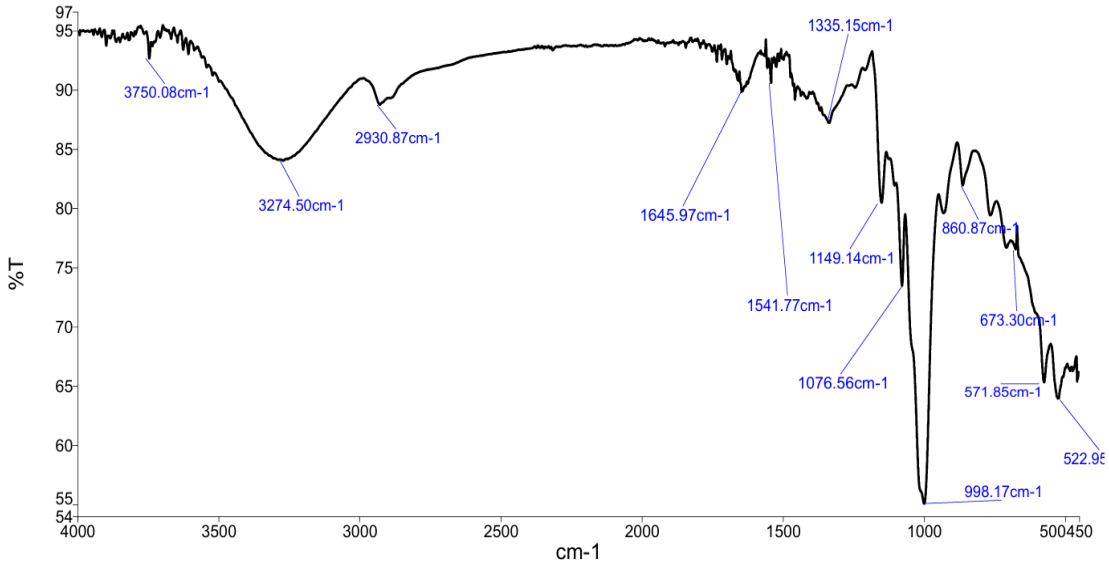

Figure 1: FT-IR spectra of pulverized cassava peels starch

The FT-IR analysis of cassava peels starch depicted in Figure 1 revealed prominent peaks at 3750.08 cm^{-1} and 3274.50 cm^{-1} corresponding to O-H stretching, indicating the presence of hydroxyl groups in cellulose, starch, and lignin. The absorption spectrum at 2930.87 cm^{-1} corresponds to C-H stretching which indicates the presence of aliphatic components in the cassava peels. The absorption peaks at 1645.97 cm^{-1} and 1541.77 cm^{-1} are attributed to the stretching of carbonyl (C=O) groups, which can be found in carboxyl groups present in cassava peels. The presence of absorption peaks at 1149.14 cm^{-1}, 1076.56 cm^{-1} and 998.17 cm^{-1} are characteristic of C-O stretching common in alcohols, carboxylic acids, and polysaccharides. The characteristic peaks at 860.87, 673.30, 571.85 and 522.95 cm^{-1} suggests Fingerprint regions vibration, which are related to aromatic ring deformation of the lignin structure (De-la-pava et al., 2023; Kayiwa et al., 2021).

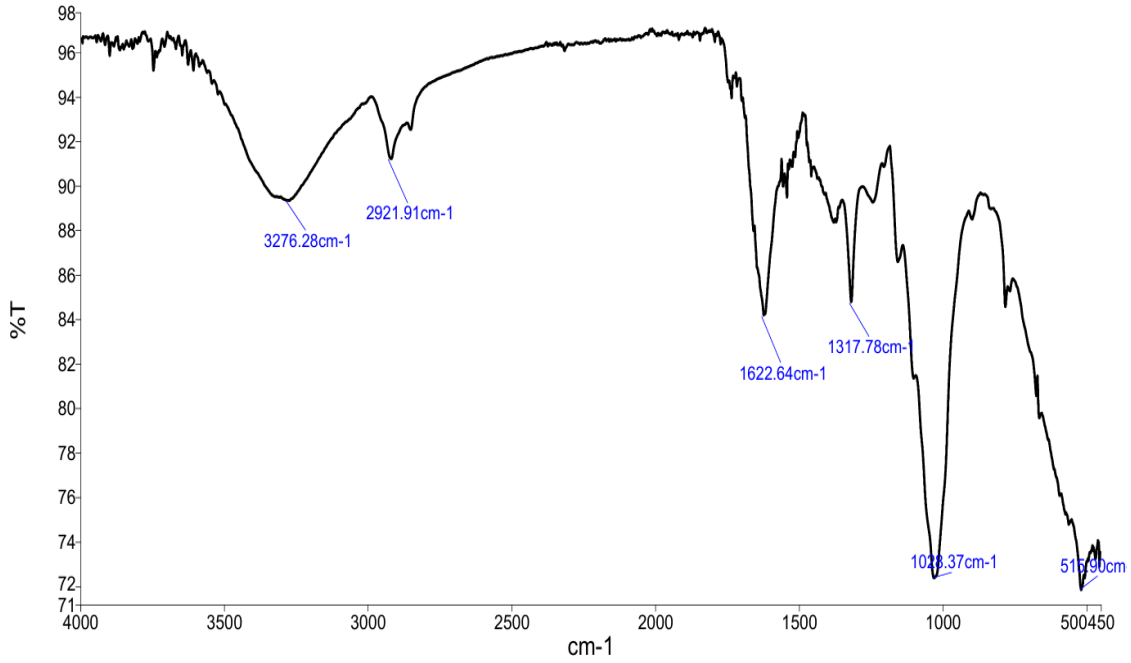

Figure 2: FT-IR spectra of pulverized plantain stem fibres

FTIR analysis of plantain stem fibre (shown in Figure 2) revealed major functional groups which provide information about the fibre's composition. Thus, the absorption peak at 3276.28 cm^{-1} corresponds to O-H stretching vibrations, indicating the presence of hydroxyl groups from cellulose, hemicellulose and lignin. The peak at 2921.91 cm^{-1} ia attributed to C-H stretching, also found in cellulose, hemicellulose, and lignin. The absorption peak at 1721.12 cm^{-1} is characteristic of a C=O (carbonyl) group, often associated with hemicellulose. The FT-IR absorption peak at 1622.64 cm^{-1} suggests C=C stretching from aromatic compounds, a component of lignin. The intensity of the peaks at 1317.78 cm^{-1} and 1025 cm^{-1} characterized by C-O and C-O-C stretches, respectively, can be related to the presence of lignin, hemicellulose, and cellulose (Adeniyi et al., 2019).

3.3 Differential Scanning Calorimetry and Thermogravimetric Analysis Results

Result of the differential scanning calorimetry (DSC) and thermogravimetric analysis (TGA) conducted on the pulverized cassava peels starch are presented in Figure 3. The DSC analysis was undertaken to enable determination of the melting temperature of cassava peels starch. For in-depth analysis on the decomposition of the pulverized cassava peels starch, the TGA thermogram was plotted to clearly reveal the steps involved in the decomposition of the pulverized cassava peels.

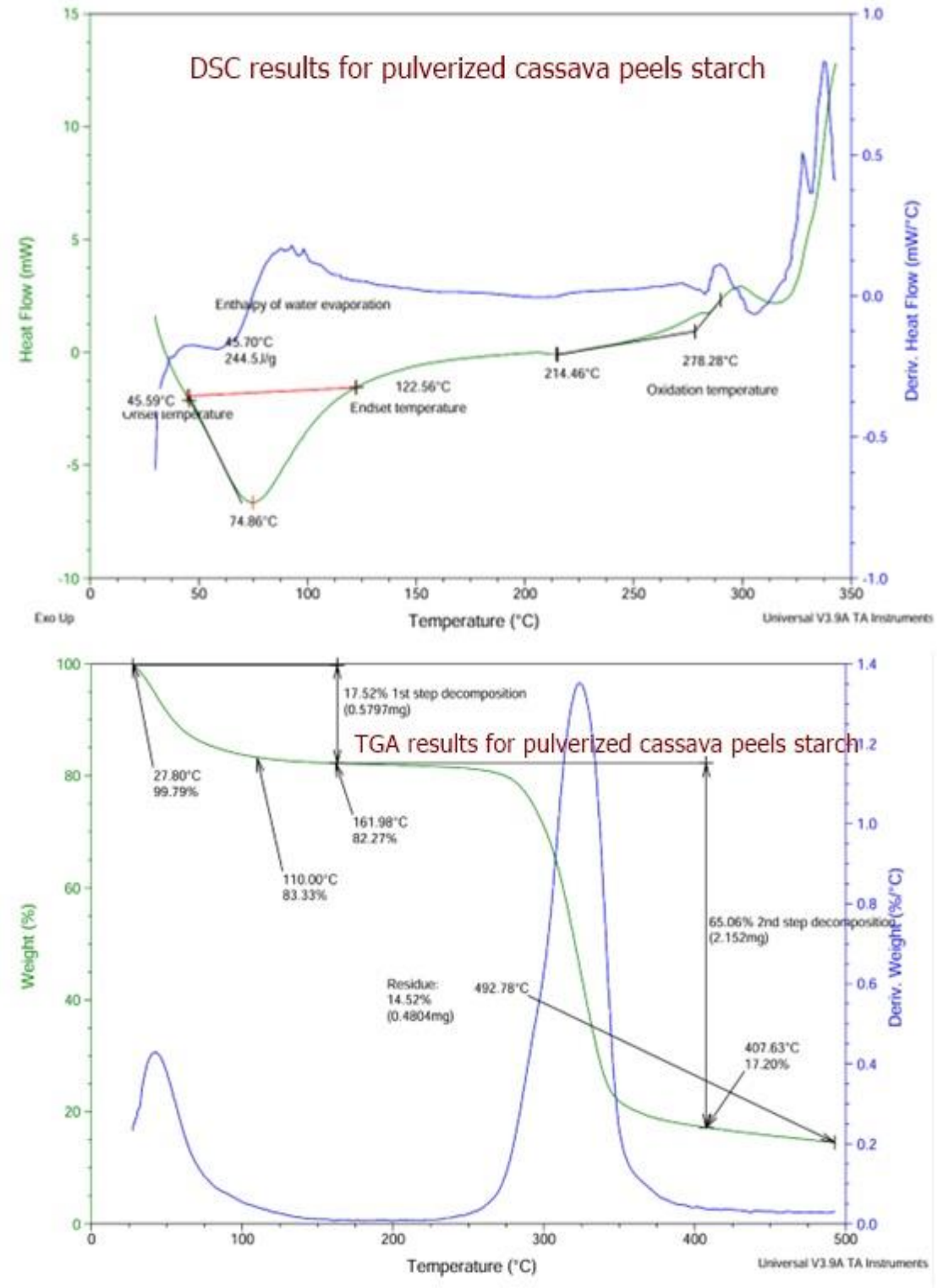

Figure 3: DSC and TGA results for pulverized cassava peels starch

The DSC analysis was undertaken to enable determination of the melting temperature of cassava peels. From the Figure 3, the melting temperature of cassava peel was observed to be 74.86 ^{o}C. Further, thermogravimetric analysis (TGA) of cassava peel was conducted to measure its weight loss as a function of temperature, revealing information about its thermal stability, moisture content, and volatile matter. Thus, the TGA thermogram was plotted and presented in Figure 3 to clearly reveal the steps involved in the decomposition of the pulverized

cassava peels. The first step decomposition phase occurred between 27.80 and 161.98 ^{o}C, where evaporation of water (dehydration) took place. The second step decomposition occurred between 161.98 and 407.63 ^{o}C, where degradation of hemicellulose and cellulose occurred. In this step, there was a significant mass loss of 2.152 mg corresponding to 65.06 %. Finally, the degradation of lignin occurred between 407.63 and 492.78 ^{o}C. This phase involved the breaking of chemical bonds and the formation of ash residue. This implies that the cassava peel powder has high thermal stability.

The DSC thermogram for plantain fibres is given in Figure 4. From the Figure 4, the water evaporation from plantain fibres occurred at 59.67 ^{o}C. Meanwhile, plantain fibre, a lignocellulosic material does not have a melting temperature but instead decomposes at high temperatures, due to its main components of cellulose, hemicellulose, and lignin. Thus, the decomposition temperature of hemicellulose and cellulose content of plantain fibres was observed at 185.27 ^{o}C. This implies that at 185.27 ^{o}C, the hemicellulose and cellulose contents of plantain fibres would be degraded. Therefore, any property that depends on hemicellulose and cellulose contents of the plantain fibres will not be operational beyond this temperature.

But closer observation of the thermogram shows that beyond the endothermic peak at 185.27 ^{o}C, no other peak was observed. The implication is that the lignin content of plantain fibre which degrade at temperatures higher than the degradation temperature of hemicellulose and cellulose is intact. Hence, the lignin content of the plantain fibre did not degrade, and therefore any property that depends on the lignin content of the plantain fibre can withstand temperature of 185.27 ^{o}C, since the function of lignin in plantain fibres is to provide structural integrity, stiffness, and compressive strength.

The TGA plot with corresponding DTG plot of plantain fibres are also presented in Figure 4. The first decomposition phase where moisture and light volatile compounds were removed occurred from 36.40 to 160.52 °C with 0.1672 mg mass loss corresponding to 6.272 % of the total mass. Between 160.52 and 397.60 °C, the slope of TGA curve indicate a significant change, and it is referred to as the second decomposition phase. Thus, there was a substantial loss of some structural composition of the plantain fibre such as volatile hydrocarbons, cellulose, and hemicellulose due to dissociation and decomposition of the molecular bonds (Subramanian et al., 2020). The mass loss due to the second decomposition is 1.537 mg which corresponds to 57.64 % of the total mass. The observed mass loss is in accordance with an established fact that during degradation of plantain fibre, loss of hemicellulose occurs first at lower temperature, followed by loss of cellulose which occurs at mid temperature.

Further, beyond the second decomposition step, there was another decomposition that occurred between 397.60 and 812.24 °C. This is called the third decomposition phase where degradation of lignin occurred.

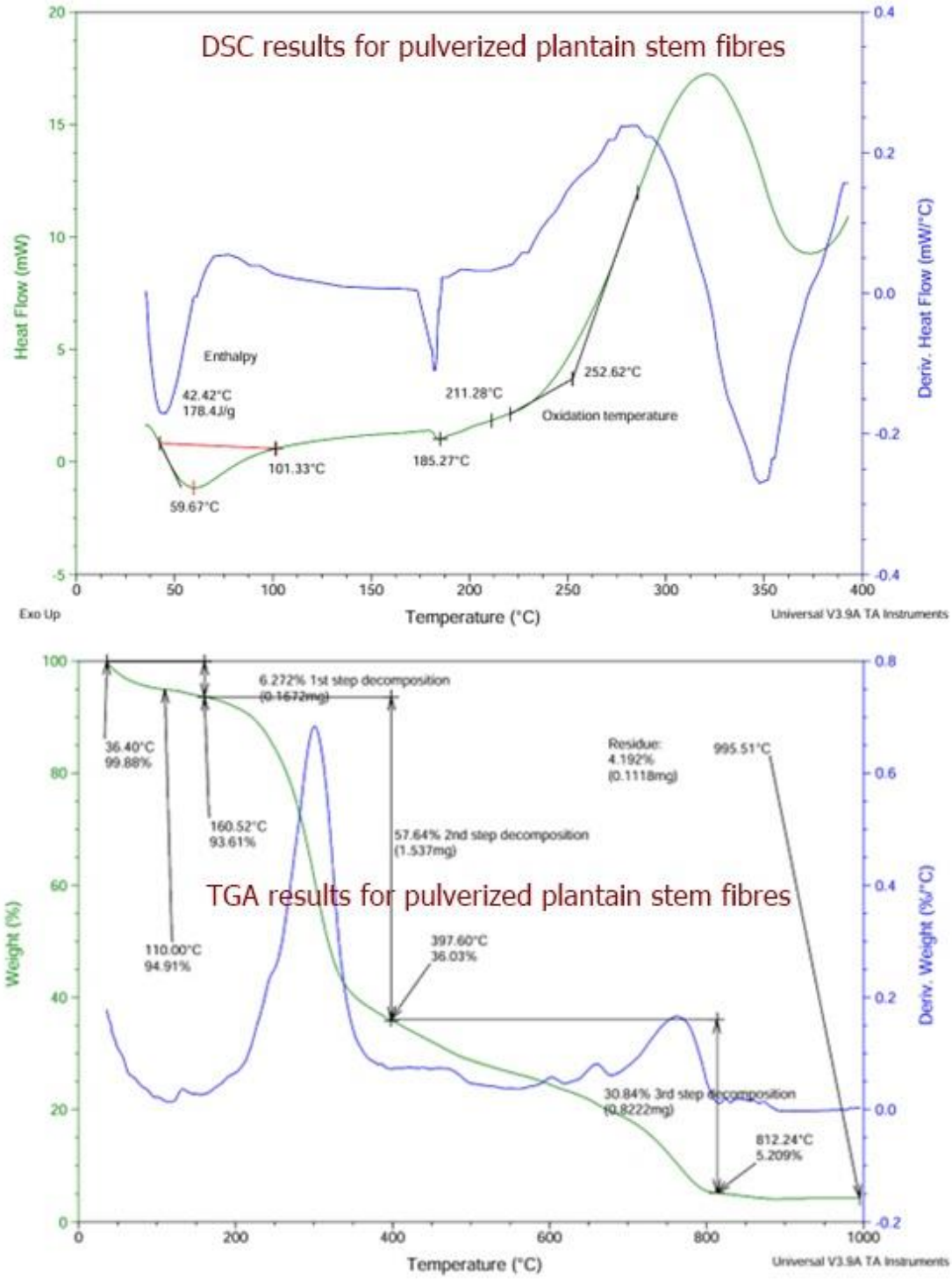

Figure 4: DSC and TGA results for pulverized plantain stem fibres

3.4 Results of the production of composite samples

Plate 3 shows the different samples of composites produced using the formulations given in Table 1. Visual observation of the virgin sample (100 LDPE) clearly confirms there is no other constituent material. A cursory look at the composite samples confirms presence of pulverized cassava peels starch and plantain stem fibres in the LDPE matrix. However, the shape of the samples produced was circular as shown in Plate 3. The average thickness of the flat circular samples was determined to be 5.80 mm.

Plate 3: Produced samples of the composite.

3.5 Results of Microstructure Analysis

Figure 5 shows the microstructural examinations of the tensile fractured virgin LDPE, 100 LDPE+100 CS+2 GA, 100 LDPE+100 CS+10 PF+2 GA, 80 LDPE+100 CS+20 PF + 2 GA, 60 LDPE+100 CS+40 PF + 2 GA and 50 LDPE+100 CS+50 PF + 2 GA. From the Figure 5, it could be clearly observed that the virgin sample is plain with characteristic lustre of polymeric matrix. The sample with 100 LDPE+100 CS+2 GA reveals sparse presence of cassava peels starch held together by gum Arabic within the LDPE polymer matrix. The sample with 100 LDPE+100 CS+10 PF+2 GA shows dense presence of the fillers bound by the gum Arabic within the polymer matrix. However, some voids were observed in samples 80LDPE+100CS+20PF+2GA and 60LDPE+100CS+40 PF+2GA which was due to pull off during tensile fracture. Again, one can see presence of fibrous fillers in samples 50 LDPE+100 CS+50 PF+2 GA. A closer observation shows that the gum Arabic could not bind the fillers together.

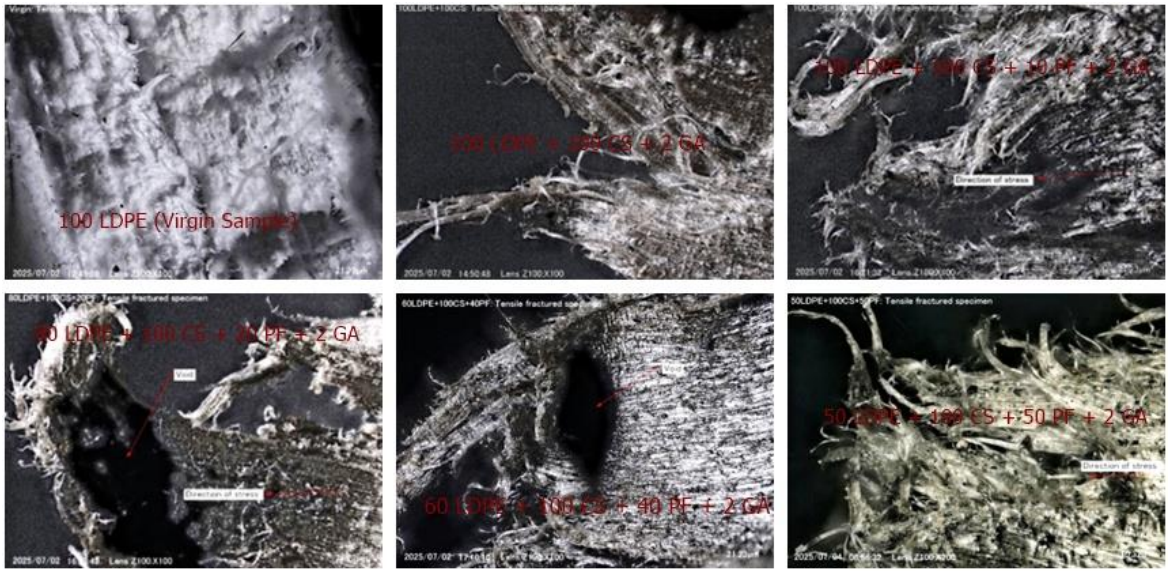

Figure 5: Microstructural examinations of the tensile fractured virgin LDPE, 100 LDPE+100 CS+2GA, 100 LDPE+100CS+10PF+2GA, 80 LDPE+100 CS+20 PF+2GA, 60 LDPE+100 CS+40 PF+2GA, 50 LDPE+100 CS+50 PF+2 GA.

3.7 Results of Mechanical Properties Analysis

(a) Tensile properties

The stress-strain curves for the virgin LDPE and composite samples are given in Figure 6. From the plots, the values of ultimate tensile strength (UTS), yield strength, Young's modulus of elasticity, and % elongation at break were determined. It is important to note that high ultimate tensile strength (UTS) signifies a material's ability to withstand large amounts of stress before failing, crucial for applications with heavy loads. Conversely, low UTS indicates a material's low fracture toughness, making it unsuitable for high-stress situations but potentially useful for applications requiring flexibility. The virgin sample has the highest UTS value. With inclusion of plantain stem fibres, the UTS values for the composite samples decreased.

Yield strength value is the point where a material transitions from elastic behavior to plastic behavior.

Therefore, high yield strength is significant for packaging materials needing rigidity and load-bearing capacity, preventing permanent deformation under stress, but it can decrease ductility and increase brittleness. Low yield strength indicates greater ductility and toughness. The high yield strength of 10.360 MPa exhibited by the virgin sample indicate that it could be rigid, with reduced ductility and increased brittleness. However, the composite samples exhibited yield strength between 4 and 6 MPa, suggesting higher ductility and toughness.

A high Young's modulus of elasticity indicates a stiff material that resists deformation, which is ideal for rigid structures, while a low Young's modulus of elasticity indicates a flexible material that easily deforms. Thus, Figure 6 presents 94.445 MPa value for the Young's modulus of elasticity of the virgin sample. Considering the Young's modulus for the composite samples, the obtained values reveal they are neither flexible nor rigid, meaning they exhibit mid-range properties.

Determination of elongation at break is a measure of durability and optimal performance of materials. From the obtained results in Table 4.9, it is clear that the virgin sample has low elongation at break. The virgin LDPE sample displayed low elongation at break. The 80 LDPE+100 CS+20 PF+2 GA composite sample exhibited the highest elongation at break, and therefore implies that it is most ductile and flexible. The 50 LDPE+100 CS+50 PF+2 GA sample also exhibited high elongation at break.

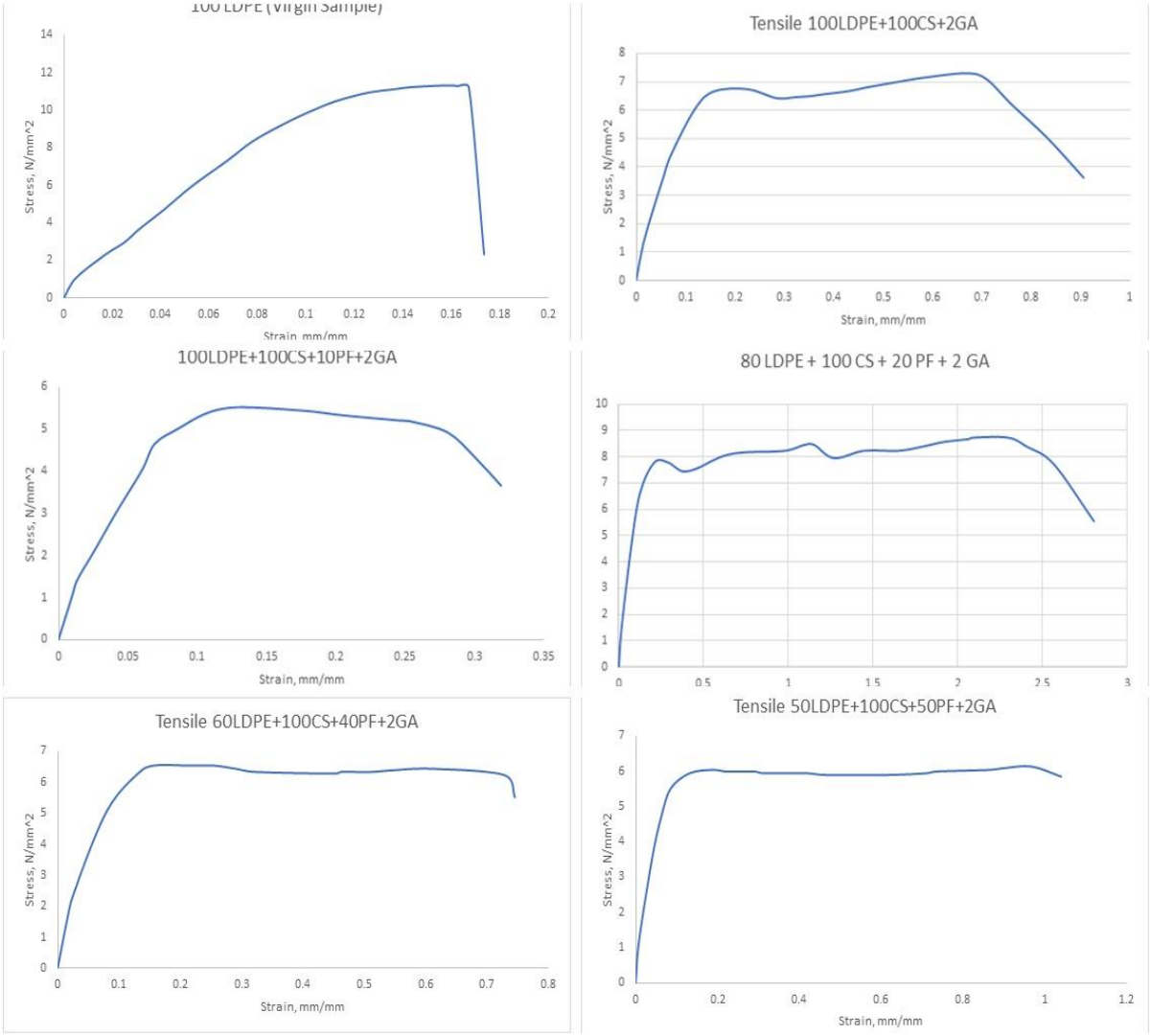

Figure 6: Plots of stress-strain curve for virgin LDPE and the composite samples

Table 4: Values of tensile properties for the bioplastic composite samples

S/N	Sample ID	Ultimate Tensile Strength (UTS), MPa	Yield Strength, MPa	Young's Modulus of Elasticity, MPa	% Elongation at Break
1	100 LDPE (Virgin Sample)	11.321	10.360	94.445	17.354
2	100 LDPE + 100 CS + 2 GA	7.298	6.070	50.675	90.553
3	100 LDPE+100 CS+10 PF+2 GA	5.519	4.667	67.092	31.933
4	80 LDPE+100 CS+20 PF + 2 GA	8.722	7.778	37.278	280.148
5	60 LDPE+100 CS+40 PF + 2 GA	6.531	6.224	48.545	74.556
6	50 LDPE+100 CS+50 PF + 2 GA	6.143	5.524	64.418	103.925

(b) Results of Compressive strength, Flexural strength and Shore D Hardness tests

The compressive strength is significant because it determines the materials' ability to withstand compressive forces exerted during packaging. Thus, Table 5 presents results of the compressive strengths for the virgin sample and composite samples. The virgin sample exhibited highest compressive strength. Notwithstanding, the composite samples displayed relatively high compressive strength values. The high compressive strength value observed in composite samples is due to presence of cellulose.

The flexural strength of a composite material is significant because it determines the material's ability to resist bending forces and maintain structural integrity, preventing premature failure, cracking. Thus, Table 5 presents values of the flexural strengths for the virgin LPDE and composites samples. A cursory look at the results reveals that the virgin sample exhibited the highest flexural strength. Considering the composites, the samples exhibited relatively high flexural strength values. The observed high flexural strength value is attributed to high flexural strength of cellulose present in cassava peels starch and plantain fibres.

Measuring a material's hardness is important because it determines a material's resistance to scratching, indentation, and wear, which directly correlates to its durability and performance. Therefore, Table 5 presents Shore D Hardness values for the virgin LDPE and composite samples. The observed results revealed that the virgin sample exhibit highest value of hardness. Considering the composites, the hardness values fall within the range of 42 and 49, which is relatively good. Thus, the hardness values of the composites indicate that they could resist scratching and wear during packaging applications.

Table 5: Values of compressive strengths for the bioplastic composite samples

S/N	Sample ID	Compressive Strength (MPa)	Flexural Strength (MPa)	Shore D Hardness
1	100 LDPE (Virgin Sample)	25.767	25.015	52
2	100 LDPE + 100 CS + 2 GA	18.951	16.479	46
3	100 LDPE + 100 CS + 10 PF + 2 GA	17.572	15.278	46
4	80 LDPE + 100 CS + 20 PF + 2 GA	19.461	16.923	42
5	60 LDPE + 100 CS + 40 PF + 2 GA	20.438	17.772	46
6	50 LDPE + 100 CS + 50 PF + 2 GA	18.448	16.042	48

3.8 Thermal Property Analysis – Linear Coefficient of Thermal Expansion

The coefficient of thermal expansion (CTE) is a measure of how much a material expands or contracts in response to a change in temperature, and is crucial for ensuring product integrity, safety, and quality by predicting dimensional changes that can lead to leakage, structural failure, or seal breaches during storage and transport. A high CTE means the material changes significantly in size with temperature. A low CTE is good for packaging applications because it ensures that the packaging maintains its shape and size even when subjected to varying temperatures during processing, shipping, and storage. It also ensures seal integrity and product protection because the material is more dimensionally stable.

Thus, Table 6 presents the CTE values of the virgin LDPE sample and those of the composite samples. From the obtained results, the LDPE virgin sample exhibited the highest coefficient of thermal expansion. For the composite samples, the CTE values were found to be quite lower, and therefore implies that it could serve veritably as packaging materials.

Table 6: Values of linear coefficients of thermal expansion for the bioplastic composite samples

S/N	Sample ID	Linear Coeff. of Thermal Expansion ($1/^{o}C$)
1	100 LDPE (Virgin Sample)	72.063×10^{-06}
2	100 LDPE + 100 CS + 2 GA	34.841×10^{-06}
3	100 LDPE + 100 CS + 10 PF + 2 GA	37.841×10^{-06}
4	80 LDPE + 100 CS + 20 PF + 2 GA	14.171×10^{-06}
5	60 LDPE + 100 CS + 40 PF + 2 GA	33.892×10^{-06}
6	50 LDPE + 100 CS + 50 PF + 2 GA	32.500×10^{-06}

3.9 Results of Water and Oil Uptake Test

Fluid uptake in packaging materials can affect their performance and durability. Thus, Table 7 presents values of water and oil uptake by the virgin LDPE sample and composite samples at room temperature (25 ^{o}C) and at elevated temperature (50 ^{o}C). From the obtained results, water and oil uptake by the samples increased with increase in temperature. Comparatively, both the virgin LDPE sample and composite samples exhibited higher uptake of water than oil. This could be attributed to the hydrophilic nature of the additives in the LDPE. However, the values of both water and oil uptake are relatively low.

Table 7: Values of water and oil uptake for the bioplastic composite samples

S/N	Sample	Water uptake (%)		Oil uptake (%)	
		25 ^{o}C	50 ^{o}C	25 ^{o}C	50 ^{o}C
1	100 LDPE (Virgin sample)	2.231	3.043	2.316	2.326
2	100 LDPE + 100 CS + 2 GA	3.215	3.374	2.842	2.935
3	100 LDPE + 100 CS + 10 PF + 2 GA	3.421	3.631	2.961	3.016
4	80 LDPE + 100 CS + 20 PF + 2 GA	3.928	4.141	3.121	3.307
5	60 LDPE + 100 CS + 40 PF + 2 GA	4.173	4.243	3.285	3.428
6	50 LDPE + 100 CS + 50 PF + 2 GA	4.282	4.504	3.310	3.553

IV. Conclusion

The effects of plantain fibre on cassava starch-modified low density polyethylene composite for use as sustainable secondary packaging material have been investigated. FTIR analysis of the plantain stem fibres revealed presence of cellulose, hemicellulose, and lignin which have inherent mechanical properties. Thus, the mechanical strengths of the composites were enhanced. The DSC and TGA thermal analyses results showed that the plantain stem filler exhibited good thermal properties. It was observed that the plantain fibres did not melt but the hemicellulose and cellulose content decomposed at 185.27 ^{o}C, but the lignin did not decompose. The linear coefficient of thermal expansion (CTE) values of the composite samples were found to be quite lower as they range from 12.658 x 10^{-06} to 46.774 x 10^{-06} **/**^{o}C**,** making it less prone to expansion when heated, and contraction when cooled. This effect is due to the inclusion of plantain stem fibre particles which hindered the LDPE polymer's ability to expand freely, leading to a more dimensionally stable material.

Also, it is important to note that plantain stem fibres and cassava peels starch are known to be biodegradable. In view of these, the produced composites would be non-toxic, biodegradable and sustainable. Thus, the produced composite samples could serve veritably as secondary food packaging materials.

V. References

1. Abotbina, W., Sapuan, S. M., Ilyas, R. A., Sultan, M. T. H., Alkbir, M. F. M., Sulaiman, S., Harussani, M. M., and Bayraktar, E.. Recent Developments in Cassava (Manihot esculenta) Based Biocomposites and Their Potential Industrial Applications: A Comprehensive Review. *Materials*, 2022; *15*(19). https://doi.org/10.3390/MA15196992.
2. Adeniyi A.G., Ighalo J.O., and Onifade D.V. Production of Bio-Char from Plantain (*musa Paradisiaca*) Fibres Using an Updraft Biomass Gasifier with Retort Heating, *Combustion Science and Technology*, 2019. DOI: 10.1080/00102202.2019.1650269.
3. Afshar S.V., Boldrin A., Astrup T.F., Daugaard A.E., Hartmann N.B. Degradation of biodegradable plastics in waste management systems and the open environment: A critical review. *Journal of Cleaner Production*, 2024; 434. https://doi.org/10.1016/j.jclepro.2023.140000.
4. Aliotta L., Gigante V., Coltelli M.B., Cinelli P., Lazzeri A. Evaluation of mechanical and interfacial properties of bio-composites based on poly (lactic acid) with natural cellulose fibres. Int. J. Mol. Sci. 2019, 20, 960.
5. Ashok A., Rejeesh C., Renjith R. Biodegradable polymers for sustainable packaging applications: A review. IJBB 2016; 1, 11.

6. Attaran S.A., Hassan A., Wahit M.U. Materials for food packaging applications based on bio-based polymer nanocomposites: A review. *J. Thermoplast. Compos. Mater*. 2015; 30, 143–173.
7. Becerra, V.; Odermatt, J. Direct determination of cationic starches in paper samples using analytical pyrolysis. *Journal of Analytical and Applied Pyrolysis*, 2013, 105(2). DOI:10.1016/j.jaap.2013.11.024.
8. Cazón P., Velazquez G., Ramírez J.A., Vázquez M. Polysaccharide-based films and coatings for food packaging: A review. *Food Hydrocoll*. 2017; 68, 136–148.
9. Dasumiati, Saridewi N., and Malik M. Food packaging development of bioplastic from basic waste of cassava peel (manihot uttilisima) and shrimp shell. IOP Conf. Series: *Materials Science and Engineering*, 2019, 602:012053. Doi:10.1088/1757-899X/602/1/012053.
10. De Kock L., Sadan Z., Arp R., Upadhyaya P. A circular economy response to plastic pollution: Current policy landscape and consumer perception. *S. Afr. J. Sci*. 2020; 116, 1–2.
11. De-la-pava R., Gómez-García M.C., Albis A.R. Gold recovery in aqueous medium by cassava peels (Manihot esculenta) modified with citric acid. *Revista EIA*, 2023; 20(39):1-20Reia3907. https://doi.org/10.24050/reia.v20i39.1612.
12. Gómez-Bachar L., Vilcovsky M., González-Seligra P., Famá L. Effects of PVA and yerba mate extract on extruded films of carboxymethyl cassava starch/PVA blends for antioxidant and mechanically resistant food packaging. *Int. J. Biol. Macromol*. 2024, 268, 131464.
13. Gruji´c R., Vujadinovi´c D., Savanovi´c D. Biopolymers as Food Packaging Materials. In Advances in Applications of Industrial Biomaterials; *Springer: Cham, Switzerland*, 2017; 139–160.
14. Hijosa-Valsero M., Paniagua-García A.I., Díez-Antolínez R. Industrial potato peel as a feedstock for biobutanol production, *New Biotechnology*, 2018; 46, 54-60. https://doi.org/10.1016/j.nbt.2018.07.002.
15. Kayiwa R., Kasedde H., Lubwama M., and Kirabira J.B. Mesoporous activated carbon yielded from pre-leached cassava peels. Bioresour. Bioprocess., 2021; 8:53. https://doi.org/10.1186/s40643-021-00407-0.
16. Khalil H.A., Davoudpour Y., Saurabh C.K., Hossain M.S., Adnan A., Dungani R., Paridah M., Sarker M.Z.I., Fazita M.N., Syakir M. A review on nanocellulosic fibres as new material for sustainable packaging: Process and applications. *Renew. Sustain. Energy Rev.* 2016; 64: 823–836.
17. Marsh K.., Bugusu B. Food packaging - roles, materials, and environmental issues. Journal of Food Science, 2007; 72(3), R39-R64.
18. Matheus J.R., de Farias P.M., Satoriva J.M., de Andrade C.J., Fai A.E. Cassava starch films for food packaging: Trends over the last decade and future research. *Int. J. Biol. Macromol*. 2023, 225, 658–672.
19. Mueller E., Hoffmann T.G., Schmitz F.R., Helm C.V., Roy S., Bertoli S.L., de Souza C.K. Development of ternary polymeric films based on cassava starch, pea flour and green banana flour for food packaging. *Int. J. Biol. Macromol*. 2024, 256, 128436.
20. Muller J., Martínez C.G., Chiralt A. Combination of poly (lactic) acid and starch for biodegradable food packaging. *Materials,* 2017; 10, 952.
21. Nurul M.F., Jayaraman K., Bhattacharyya D., Mohamad M.H., Saurabh C.K., Hussin M.H., HPS A.K. Green composites made of bamboo fabric and poly (lactic) acid for packaging applications—A review. *Materials*, 2016; 9, 435.
22. Peelman N., Ragaert P., De Meulenaer B., Adons D., Peeters R., Cardon L., Van Impe F., Devlieghere F. Application of bioplastics for food packaging. Trends Food Sci. Technol. 2013; 32, 128–141.
23. Rundh B. The multi-faceted dimension of packaging. *British Food Journal*, 2005; 107(9), 670-684.
24. Scarfato P., Di Maio L., Incarnato L. Recent advances and migration issues in biodegradable polymers from renewable sources for food packaging. *J. Appl. Polym. Sci.* 2015; 132, 13.
25. Silayoi P., Speece M. The importance of packaging attributes: A conjoint analysis approach. *Journal of Food Products Marketing*, 2007; 13(2), 1-18.
26. Subramanian, P., Gitanjali, J., Nithya, K., & Prabha, B. (2020). Investigation on thermal degradation of bamboo (*Bambusa vulgaris*) culm at varied heating rates through TG analyzer. *International Journal of Chemical Studies, 8*(4), 3881–3883.
27. Zhang Y., Xie J., Ellis W.O., Li J., Appaw W.O., Simpson, B.K. Bioplastic films from cassava peels: Enzymatic transformation and film properties. *Ind. Crops Prod*. 2024, 213, 118427.